Dalton Transactions

Accepted Manuscript

This is an *Accepted Manuscript*, which has been through the Royal Society of Chemistry peer review process and has been accepted for publication.

Accepted Manuscripts are published online shortly after acceptance, before technical editing, formatting and proof reading. Using this free service, authors can make their results available to the community, in citable form, before we publish the edited article. We will replace this *Accepted Manuscript* with the edited and formatted *Advance Article* as soon as it is available.

You can find more information about *Accepted Manuscripts* in the Information for Authors.

Please note that technical editing may introduce minor changes to the text and/or graphics, which may alter content. The journal's standard Terms & Conditions and the Ethical guidelines still apply. In no event shall the Royal Society of Chemistry be held responsible for any errors or omissions in this *Accepted Manuscript* or any consequences arising from the use of any information it contains.

ROYAL SOCIETY OF CHEMISTRY

www.rsc.org/dalton

Imidazole derivative-functionalized carbon dots: Using as a fluorescent probe for detecting water and imaging of live cells

Xudong Wang[a], Dan Wang[a], Yali Guo[a], Chengduan Yang[a], Anam Iqbal[a], Weisheng Liu[a], Wenwu Qin[a], Dan Yan[b], Huichen Guo[b**]*

[Jan 12, 2015]

[a]*Key Laboratory of Nonferrous Metal Chemistry and Resources Utilization of Gansu Province and State Key Laboratory of Applied Organic Chemistry, College of Chemistry and Chemical Engineering, Lanzhou University, Lanzhou 730000, P. R. China.*

[b]*State Key Laboratory of Veterinary Etiological Biology and Key Laboratory of Animal Virology of Ministry of Agriculture, Lanzhou Veterinary Research Institute, Chinese Academy of Agricultural Sciences, Xujiaping 1, Lanzhou, Gansu, 730046, The People's Republic of China*

Abstract

A highly sensitive for water fluorescence carbon dots-imidazole (CDs-imidazole) nano probe is prepared through covalently conjugating imidazole group onto the surface of carbon dots. In organic solvents, quenching of fluorescence occurs via photoinduced electron transfer (PET) process from the imidazole nitrogen to CDs

* Corresponding author: Fax: +86-931-8912582 E-mail address: qinww@lzu.edu.cn (W. Qin); ghch-2004@hotmail.com (H. Guo)

Dalton Transactions Accepted Manuscript

acceptor. Addition of trace amount of water into CDs nanocomposites in various organic solvents leads to a fluorescence turn-on response, which can be attributed to suppression of PET due to the formation of the ‘‘free’’ ion pair by proton transfer from the carboxyl groups that on the CDs surface to the imidazole nitrogen through water-bridged. This phenomenon can be used for the highly selective detection of trace amount water in organic solvents. Laser confocal microscope experiment shows the potential utilization of CDs-imidazole for the probed proton-transfer reactions in living cells.

1. Introduction

Carbon nanomaterials have drawn increasing attention because of their valuable qualities. These materials primarily include carbon nanotube[1], fullerenes[2], graphene [3]and nanofibers[4]. Recently, there has been a new form of nanostructured carbon dots (CDs), consist of a fascinating class of recently discovered nanocarbons displaying excitation wavelength-dependent photoluminescence (PL) properties, photostability, the small size, water solubility, biocompatibility and excellent cell membrane permeability. Due to the potential environmental and biological hazards of the traditional semiconductor quantum dots (QDs)[5], the CDs are attracting considerable attention as a promising alternative compared to semiconductor QDs. When it comes to the synthetic aspect, CDs can be obtained by two main approaches “top-down” and “bottom-up”[6]. Top-down approaches involve arc discharge[7], laser ablation[8], and electrochemical oxidation[9], where the CDs are formed or “broken off” from a larger carbon structure. Bottom-up approaches involve, for example,

Dalton Transactions Accepted Manuscript

combustion/thermal[10, 11], supported synthetic[12], or microwave methods[13, 14] during which the CDs are formed from molecular precursors.

Due to the excellent properties, CDs are versatile and tunable surface functionalities, which can be used in a wide range of technologies, such as bioimaging[15-17], catalysis[9, 18], biosensing[19-21], optoelectronic devices[22]. Recently, through surface functionalization, CDs have been endowed with molecular recognition ability and applied in chemical sensing. Dong et al[23] have developed polyamine-functionalized C-dots and used them for selective detection of Cu^{2+}. Shi et al[24] have developed fluoresceinisothiocyanate and rhodamine B isothiocyanate-functionalized CDs and used them for a tunable ratiometric fluorescent pH CDs.

The qualitative and quantitative detection of low-level water content as impurity in organic solvents is of great significance in several of chemistry and industrial process such as pharmaceutical manufacturing, food processing, paper production, biomedical and environmental monitoring[25]. Recently, optical water sensors[26, 27] based on fluorescence intensity and absorption appear to be particularly attractive on account of their highly sensitive and selective, quick, inexpensive, easy to fabricate, and non-destructive properties as well as their capability of remote and in situ monitoring of optical measurements.

Imidazole/imidazolium with its favorable pKa was served as pH-sensitive function group for the near-neutral pH range. In a previous paper, we reported the near-neutral BODIPY–imidazole pH indicator[28] .

Dalton Transactions Accepted Manuscript

In this paper, CDs-imidazole nano material is developed through covalently conjugating 1H-Imidazole-4-carboxylic acid onto the surface of CDs using carbodiimide chemistry. [29] The fluorescence property of CDs-imidazole nano material is not only sensitive to proton but also for water. To the best of our knowledge, a highly sensitive fluorescence PET water probe based on CDs nearly has so far been unexplored.

2. Experimental section

2.1 Chemicals

Urea, anhydrous citric acid and *p*-Toluenesulfonic acid monohydrate (*p*TsOH, 99%) were purchased from Guangfu Reagent Company (Tianjin, China). 1H-Imidazole-4-carboxylic acid and thionyl chloride were purchased from Energy chemical (Shanghai, China). All solvents and reagents were of analytical grade. Acetonitrile (MeCN), THF and ethanol (EtOH) were dried before used.

2.2 Instrument

^{1}H NMR spectra was taken on a Bruker DRX-400 spectrometer with TMS as the internal standard and D_2O as the solvent. XRD measurements were performed on a X-ray diffractometer (D/max-2400pc, Rigaku, Japan) with Cu Kα radiation (λ = 1.54178 Å), with operating voltage and current at 40 kV and 60mA, respectively. The 2θ range was from 10°to 80° in steps of 0.02°. FT-IR spectra were conducted within the 4000–400 cm^{-1} wavenumber range using a Nicolet 360 FTIR spectrometer with the KBr pellet technique. The transmission electron microscopy (TEM) was taken on a JEOL JEM2100 TEM instrument at an accelerating voltage of 200 keV. Dynamic

Dalton Transactions Accepted Manuscript

light scattered (DLS) was got on a BI-200SM (USA Brookhaven) at room temperature. Elemental analysis was obtained by a Vario cude (Germany).

2.3 Steady-state UV–vis absorption and fluorescence spectroscopy

UV–vis absorption spectra were recorded on a Varian UV-Cary100 spectrophotometer, and for the corrected steady-state fluorescence emission spectra, a FLS920 spectrofluorometer was employed.

Quantum yields were determined by an absolute method using an integrating sphere based upon that originally developed by de Mello et al[30].

2.4 Time-Resolved Fluorescence Spectroscopy

Fluorescence lifetimes were measured on an Edinburgh Instruments FLS920 equipped with the light emitting diodes (excitation wavelength 360 nm), using the time-correlated single photon counting technique [31-33] in 2048 channels at room temperature. The samples were dissolved in water and the concentrations were adjusted to have optical densities at the excitation wavelength (360 nm) < 0.1. The monitored wavelengths were 440 nm, 460nm, and 480 nm.

Histograms of the instrument response functions (using a LUDOX scatter) and sample decays were recorded until they typically reached 1.0×10^4 counts in the peak channel. Obtained histograms were fitted as sums of the exponentials, using Gaussian-weighted nonlinear least squares fitting based on Marquardt-Levenberg minimization implemented in the software package of the instrument. The fitting parameters (decay times and preexponential factors) were determined by minimizing the reduced chi-square χ^2. An additional graphical

Dalton Transactions Accepted Manuscript

method was used to judge the quality of the fit that included plots of surfaces ("carpets") of the weighted residuals vs. channel number. All curve fittings presented here had χ^2 values < 1.1.

2.5 Synthesis of CDs

Briefly, CDs were synthesized according to a reported method.[34] First, citric acid (3 g) and urea (3 g) were added to distilled water (10 ml) to form a transparent solution. The solution was then heated in a domestic 750 W microwave oven for 4–5 mins, during which the solution changed from being a colorless liquid to a brown and finally dark-brown clustered solid, indicating the formation of Carbon dots. The solid was then transferred to a vacuum oven and heated at 60 °C for 1 h to remove the residual small molecules. An aqueous solution of the CDs was purified in a centrifuge (8000 r min^{-1}, 20 min) to remove large or agglomerated particles.

2.6 Synthesis of compound1.

100mg of 1H-Imidazole-4-carboxylic acid was dispersed in 20 ml thionyl chloride. Under nitrogen atmosphere, the mixture was stirred overnight at 80 °C and then cooled to room temperature. The residual $SOCl_2$ was distilled under reduced pressure. Compound 1 was obtained after complete distillation of the thionyl chloride.

2.7 Preparation of CDs-imidazole

To a solution of compound 1 in 20mL anhydrous THF was added 100mg CDs and stirred at 80°C for 12h under nitrogen atmosphere. After cooling to room temperature, the reaction mixture was concentrated by evaporation. And the residue

Dalton Transactions Accepted Manuscript

was centrifuged and the obtained nanoparticles were washed 5 times with ethanol and then dried for further use.

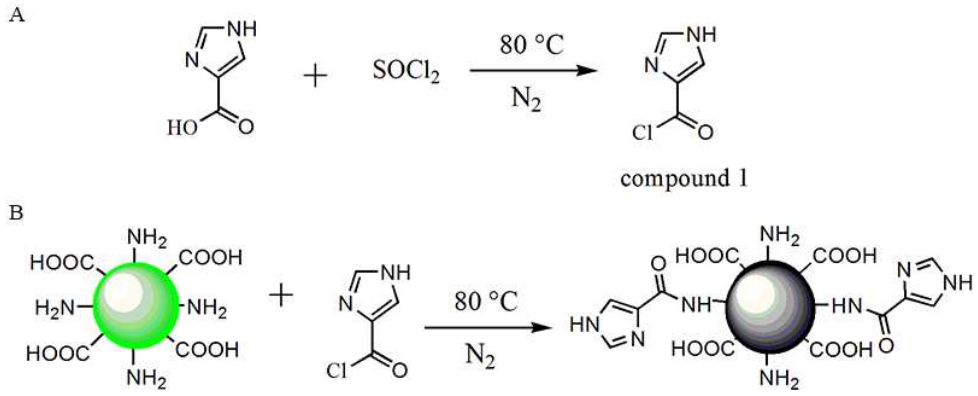

Scheme 1 Synthesis of compound 1 (a) and CDs-imidazole (b)

2.8 Cell culture, fluorescence imaging and cytotoxicity assay

Cell Culture and fluorescence imaging. Baby Hamster Syrian Kindey (BHK) cells were cultured in DMEM (Dulbecco's Modified Eagle Medium) supplemented with 10% FBS (fetal bovine serum). The cell lines were maintained in a humidified atmosphere containing 5% CO_2 at 37 °C. After removal of the culture medium, cells were incubated with CDs-imidazole (0.2 mg/ml) in 1.0 ml of fresh culture medium for 2 h. Before imaging measurement, the cells were washed three times with PBS to remove the residual nanoparticles. Cells were observed under an Olympus FV1000-IX81 laser confocal microscope.

Cytotoxicity Test. BHK Cells were seeded at a density of 10^4 cells per well (100 µl total volume/well) in 96-well assay plates for 24 h. Then, the as-prepared CDs-imidazole, at the indicated concentrations (20, 40, 80, 160, 200 $\mu g ml^{-1}$), were added to the cell culture medium. Cells were incubated with CDs-imidazole for 24 h. To determine toxicity, 3-(4, 5-Dimethylthiazol-2-yl)-5-(3-carboxymethoxyphenyl)-2-

Dalton Transactions Accepted Manuscript

(4-sulfophenyl)-2H-tetrazolium, inner salts(MTS) was added to each well of the microtiter plate and the plate was incubated in the CO_2 incubator for additional 4 h. Absorbance values were determined with Bio-Rad model-680 microplate reader at 490 nm (corrected for background absorbance at 630 nm). The cell viability was estimated according to the following equation: cell viability (%) = mean of absorbance value of treatment group/mean absorbance value of control × 100%.

3. Results and discussion

3.1 Preparation and characterization of CDs-imidazole

The proposed CDs-imidazole was fabricated as shown in Scheme1. The prepared CDs were as the platform for the proposed by one-step microwave synthesis route with critic acid and urea as the carbon source. Then, compound 1 was linked to the surface of CDs. The products were confirmed by TEM, DLS, ^{1}H NMR, XRD, elemental analysis and FTIR.

The morphology of the CDs (Fig. 1A (a)) and CDs-imidazole (Fig. 1A (b)) were characterized by transmission electron microscopy (TEM). The TEM illustrates that the CDs are spherical and well dispersed, and the average diameter of carbon dots was about 2 nm. Fig. 1A (b) shows the TEM image of the synthesized CDs-imidazole, the result revealed no obvious morphology change of CDs after the surface functionalization. Dynamic light scattering (DLS) (Fig.S1) analysis shows the average hydrodynamic diameter of CDs is about 2± 0.43 nm.

The surface functionalization processes were also characterized by XRD and elemental analysis. As shown in fig. 1B curve a, several obvious sharp strong peaks

Dalton Transactions Accepted Manuscript

(for example 18°, 22° and 28°) in the range of 2θ=15°-30° for 1H-Imidazole-4-carboxylic acid were observed. A broad peak can be observed at around 2θ=23° for carbon dots (curve b), corresponding to highly disordered carbon atoms[34]. In addition, as shown in curve c, the broad peak 23° of carbon dots, three sharp peaks (18°, 22° and 28°) of imidazole were also observed in the XRD of the CDs-imidazole, indicating the successful conjugation of imidazole onto the surface of CDs. Elemental analysis results (Table S1) indicate that both CDs and CDs-imidazole are mainly composed of carbon, nitrogen, hydrogen and oxygen. But the content of carbon in the CDs-imidazole is slightly higher than that in the CDs and the content of nitrogen is slightly lower than that in the CDs. The results indicate that the successful conjugation of 1H-Imidazole-4-carboxylic acid onto the surface of CDs.

^{1}H NMR analysis of the 1H-Imidazole-4-carboxylic acid, CDs and CDs-imidazole were performed in D_2O. As shown in fig. 1C (a), the appearance of two peaks at 7.54 and 8.48 ppm were assigned to the heteromatic rings of 1H-Imidazole-4-carboxylic acid. While, the signals of H (-CH_2- of critic acid or -NH_2)of CDs at 2.5 and 5.8 ppm were far away from those of 1H-Imidazole-4-carboxylic acid (Fig.1C (b)). From the comparison, it could be observed that the CDs-imidazole contained the characteristic peaks (2.5, 5.8, 7.55 and 8.48) of both CDs and 1H-Imidazole-4-carboxylic acid (Fig. 1C (c)). Obviously, these results were confirmed the successful of 1H-Imidazole-4-carboxylic acid onto the surface of CDs.

As shown in fig. S2, 1H-Imidazole-4-carboxylic acid, CDs and CDs-imidazole

Dalton Transactions Accepted Manuscript

was further verified by the FTIR measurements. The peaks in the range of 1407–1520 cm^{-1} were attributed to the skeletal vibration of the heteroaromatic rings (curve a). The broad band at 3421.3 cm^{-1} (ν_{N-H}) should be attributed to the vibration of $-NH_2$ groups, verifying the existence of amine groups on the surface of CDs (curve b). Compared to 1H-Imidazole-4-carboxylic acid , the presence of the peak at 1702 cm^{-1} which was observed in the spectra of both the CDs-imidazole and CDs was assigned to C=O stretching. In addition, the peaks around the range of 1407–1520 cm^{-1} originated from the heteroaromatic skeletal vibration of 1H-Imidazole-4-carboxylic acid were also observed in the FTIR spectra of the CDs-imidazole.

UV-vis absorption spectra of 1H-Imidazole-4-carboxylic acid, CDs and the CDs-imidazole in aqueous solution were carried out as shown in fig. 1D. The peak at around 228 nm and 300 nm of the 1H-Imidazole-4-carboxylic acid is due to π-π^* and σ-π^* transition of C=N.. The absorption spectrum of CDs exhibits bands at 275 nm, 340 and 420 nm. The absorption spectrum is similar to that of the CDs reported in the literature[34]. The absorption spectrum of CDs-imidazole exhibits maximum bands at around 230 nm, 275 nm and a broad band from 300-600 nm, the absorption peaks of CDs-imidazole represent a typical combination of 1H-Imidazole-4-carboxylic acid and CDs.

Dalton Transactions Accepted Manuscript

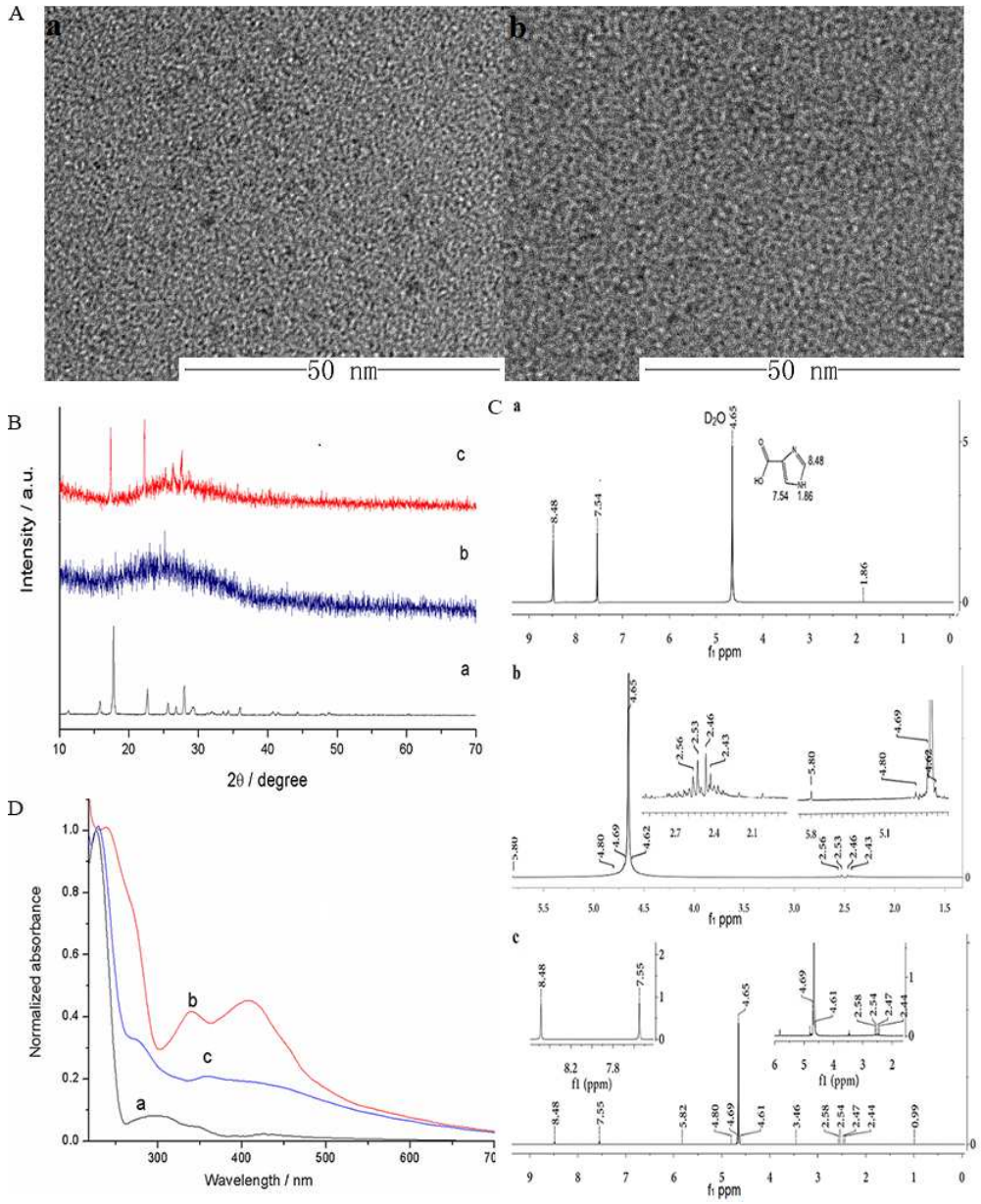

Fig. 1 (A) TEM images of the carbon dots (a) and CDs-imidazole (b). (B) XRD of 1H-Imidazole-4-carboxylic acid curve (a), CDs curve (b) and CDs-imidazole curve (c) (C) ^{1}H NMR spectrum of 1H-Imidazole-4-carboxylic acid (a), CDs(b) and CDs-imidazole (c) (D) Normalized UV-vis spectra of 1H-Imidazole-4-carboxylic acid curve (a), the CDs curve (b) and the CDs-imidazole curve (c) in water.

Dalton Transactions Accepted Manuscript

3.2 CDs-imidazole for water detection

The absorption and fluorescence spectra of CDs-imidazole were also measured in other dry organic solvents such as cyclohexane, dichloromethane, THF, ethanol and acetonitrile. As shown in fig. S3, the absorption spectra of CDs-imidazole are hardly affected by solvent, in all the organic solvents underwent no appreciable changes in shape of the peak. The absorption spectra are of similar shape as that of CDs-imidazole in water.

Contrary to the near-invariance of the absorption spectra in different solvents and water, the fluorescence emission intensity of CDs-imidazole is moderately high in water, whereas in all other solvents used the emission intensity is strongly quenched (Fig. 2). Under the ultraviolet lamp, the CDs-imidazole solution changed continuously from no fluorescence in organic solvents to strong blue green fluorescence in water as presented in the inset of fig. 2. This is attributed to an efficient quenching via photoinduced electron transfer (PET) process from the nitrogen atom of the imidazole to CDs acceptor.

Dalton Transactions Accepted Manuscript

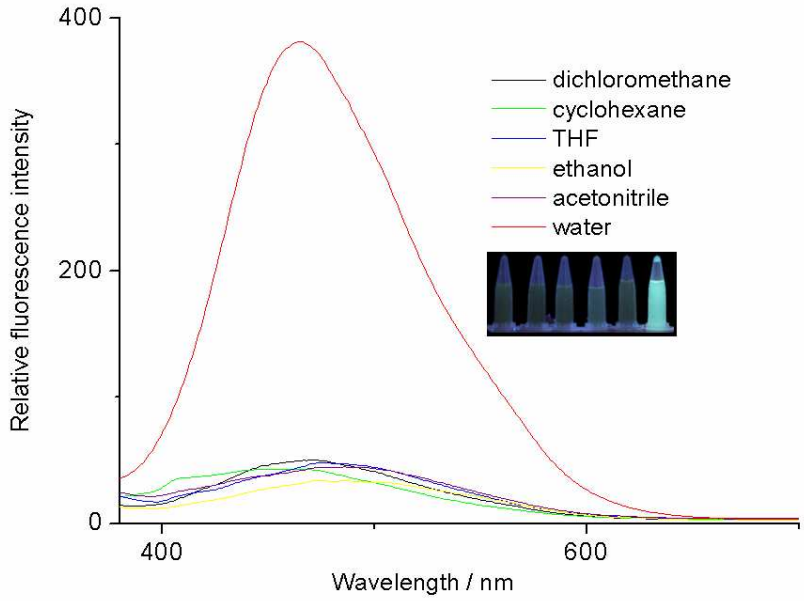

Fig. 2 Fluorescence spectra （λ_{ex}=360 nm）of the CDs-imidazole in different solvents and water. The inset shows the optical photos of the CDs-imidazole recorded at UV-lamp irradiation in different solvents and water.

It has been reported that the fluorescence emission spectra and photoluminescent intensity of CDs depend on the excitation wavelength[6]. The prepared carbon dots exhibited a bright blue-green colour under ultraviolet radiation (λ_{ex}=365 nm). The photoluminescent properties of CDs were examined in aqueous solution at several excitation wavelengths shown in fig. S4. It can be seen that, the photoluminescent emission spectra and photoluminescent intensity of CDs in water are strongly excitation wavelength dependent. The emission bands are bathochromic-shift shifted with an increase of the excitation wavelength. The strongest PL emission band with a maximum at 527 nm was observed with an excitation wavelength of 420 nm. The fluorescence spectra of carbon dots (CDs) were measured in different solvents (both organic and water) shown in Fig S5a. Both in organic solvents (EtOH, MeCN and THF) and in water, the fluorescence emission intensities of carbon dots were strong.

Dalton Transactions Accepted Manuscript

In addition of water to the in organic solvents (EtOH, MeCN and THF) will decrease The fluorescence intensity of original CDs (fig.S6)

In this contribution, PET quenched the PL of CDs-imidazole in different organic solvents. CDs-imidazole only showed stronger fluorescent in water, so photoluminescence of CDs-imidazole study was carried out in water by using different excitation wavelengths. As shown in fig. S7, the emission bands shifted with the increasing excitation wavelength, which revealed a distribution of the different surface energy traps toward the CDs[35, 36]. The maximum excitation and emission of the CDs-imidazole are located at 360 and 466 nm in water, respectively. The maximum excitation and emission of the CDs-imidazole blue-shifts about 60 nm compared to CDs.

Absorption and fluorescence properties of CDs-imidazole were measured in ethanol containing various concentrations of water. As shown in figure S8, the absorption spectra of the CDs-imidazole in ethanol underwent no appreciable changes in intensity and shape of peak upon addition of water, suggesting only weak ground state interactions.

The fluorescence emission spectra, however, change considerably, as shown in fig. S9a and fig. 3a.The fluorescence intensity of CDs-imidazole at 465 nm continuously increased with the stepwise addition of water under the excitation of 360 nm. As shown in fig. S9b and fig. 3b, the fluorescence intensity increased almost linearly with increasing water content (0-5 % and 5-20 %, v/v) in ethanol. However, the fluorescence level off and is no longer dependent on the water content once it is

Dalton Transactions Accepted Manuscript

higher than 23% (v/v). The calibration curve for water content in ethanol was obtained as shown below, where F stands for the fluorescence peak intensity in ethanol upon addition of water.

$F=3.53 \times [H_2O] +40.3$ ($r = 0.990$ $[H_2O]$ = 0-5 %, v/v)

$F= 9.71 \times [H_2O] +0.5$ ($r = 0.993$ $[H_2O]$ = 5-20 %, v/v)

The calibration equation serves as the quantitative basis for the detection of water content in ethanol. The detection limit (DL) was estimated based on the following equation: $DL = 3.3\sigma/k$, where σ is the standard deviation of the blank sample and k is the slope of the calibration curve. The DL of this water sensor was 0.28 % (0-5 %, v/v) and 0.1 % (5-20 %, v/v) for ethanol. The result indicated that the CDs-imidazole could be potentially utilized as an excellent optical sensor for the quantitative analysis of water in ethanol.

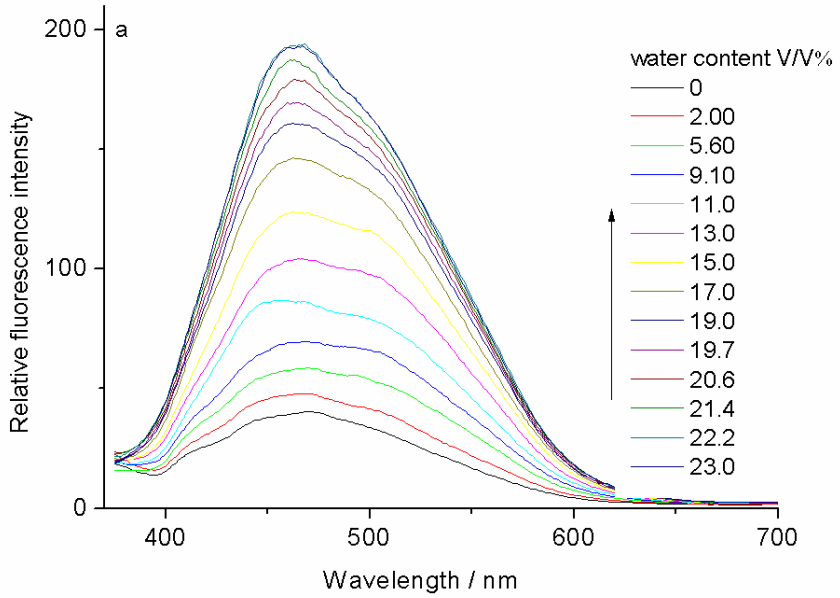

Dalton Transactions Accepted Manuscript

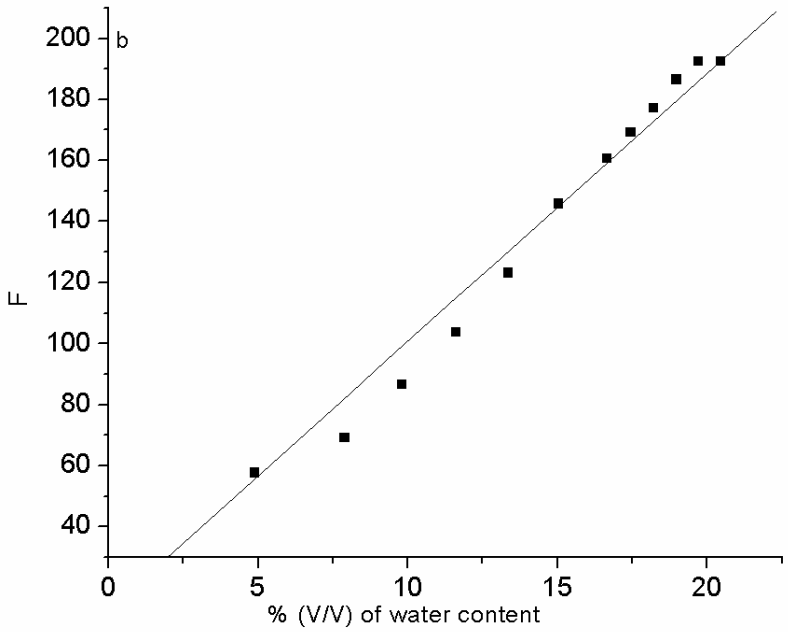

Fig. 3 Fluorescence emission spectra (λ_{ex}=360 nm) of CDs-imidazole upon in ethanol with increasing water content (0-23 %, v/v) (a) and Calibration curves as a function of water content (5-20 %, v/v) in enthanol (b).

Water has been the most widely used solvent for proton transfer studies due to its proton accepting and conducting properties and being recognized as an active participant, rather than just a passive medium in the initial deprotonation step and in the transport mechanism of the proton[37, 38]. These results indicate that the fluorescence enhancement of CDs-imidazole with the increase in the water content can be attributed to suppression of PET due to the formation of CDs-imidazole with stable fluorescent ionic structure between the protonated nitrogen atom of the imidazole (electron donor/proton acceptor) and the deprotonated carboxyl groups on the CDs (electron acceptor/proton donor) surface by hydrolysis. A simplified description of the

Dalton Transactions Accepted Manuscript

model is presented in fig. 4, where HBC is the hydrogen bonded complex, which means that the formation of "water complex". HBIP is the hydrogen bonded ion pair, SSIP is the solvent separated ion pair where the ions are separated by a few solvent molecules but are still held together by the Coulombic interactions and FIP is the fully solvated ''free'' ion pair[39]. Complexation with water leads to enhanced excited state proton transfer from the carboxyl groups that on the CDs surface to the imidazole nitrogen through water-bridged, resulting in a ''free'' ion pair. At low water concentration (0-5 % v/v) only a few water molecules are in between the -COOH and the imidazole nitrogen. At this stage, reorientation of the water molecules may still be required. Upon increasing the concentration of water proton transfer occurs more through the water bridged and the fluorescence enhancement is pronounced.

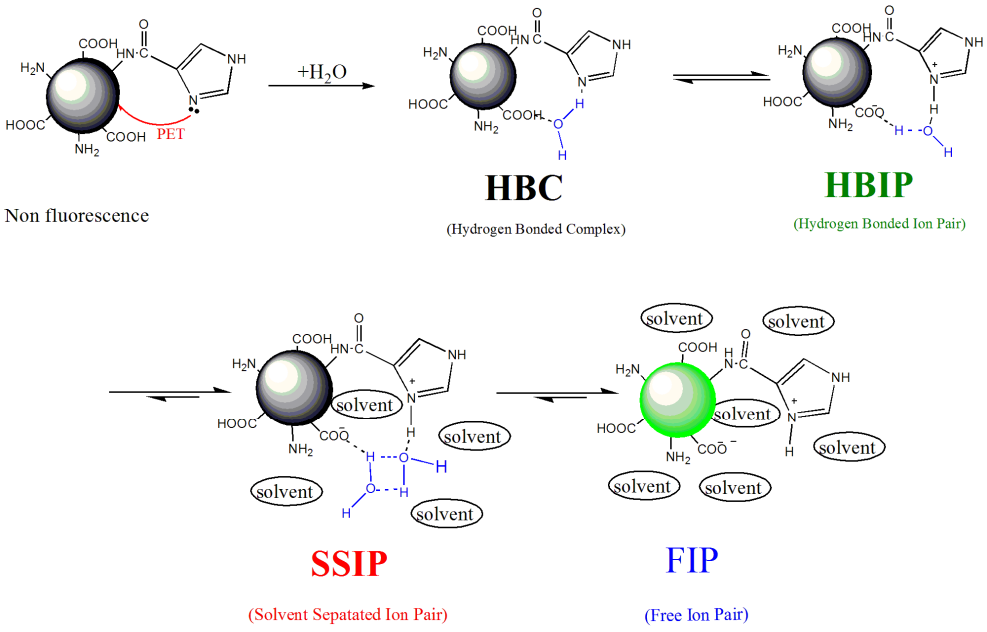

Fig. 4 Simplified reaction scheme of the excited-state free ion pair formation of CDs-imidazole in ethanol–water media.

In support of this suppress PET process, upon increasing of *p*-Toluenesulfonic

Dalton Transactions Accepted Manuscript

acid monohydrate (*p*TsOH) in ethanol, the characteristic emission band (Fig. S10) of CDs-imidazole at 465 nm was gradually increasing. This result can be attributed to the fact that protonation imidazole nitrogen suppresses PET process (it cannot donate an electron).

3.3 Cell imaging and cytotoxicity

Proton-transfer reactions are of key importance for many chemical[40, 41] and biological processes[42-44]. Subsequent experiments using a laser confocal microscope probed proton-transfer reactions in CDs-imidazole can occur or not in living cells. As shown in Fig. 5, fluorescence microscope images of BHK cells loaded with CDs-imidazole for 2h at 37 °C shows intracellular green fluorescence, suggesting that CDs-imidazole can be transfected into the living cells and applied for fluorescence imaging. Suggesting proton-transfer reactions in CDs-imidazole nano material can also take place in living cells, and emission occurs from the form of the ‘‘free’’ ion pair of CDs-imidazole.

Moreover, Cell cytotoxicity experiments of carbon dots were evaluated using BHK cell lines through the MTS assay. As shown in Fig. S11, the CDs-imidazole exhibited low cytotoxicity, which may be due to the low toxicity of CDs.

Dalton Transactions Accepted Manuscript

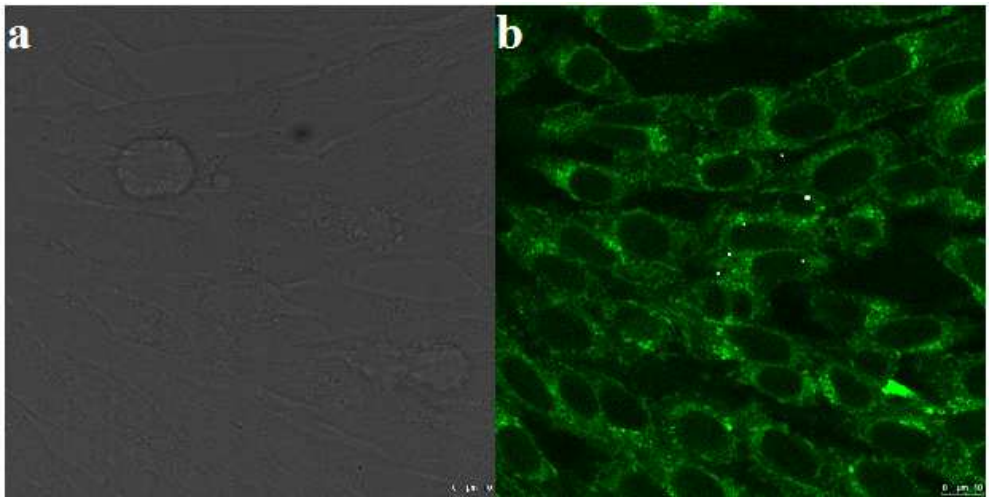

Fig.5 Fluorescence image of BHK cells incubated with 200 μg ml^{-1} of the CDs-imidazole. The bright-field images (a); the confocal fluorescence images (b).

4. Conclusions

In conclusion, a highly sensitive for water fluorescence CDs-imidazole nano probe has been prepared by conjugating imidazole group onto the surface of CDs. In organic solvents, quenching of fluorescence occurs via photoinduced electron transfer (PET) process from the nitrogen atom of the imidazole to CDs acceptor. Protonation the nitrogen atom of the imidazole by in addition of *p*TsOH in ethanol can suppresses this process. Furthermore, it was found that the CDs-imidazole shows enhancement of fluorescence with increasing water content in various solvents, which can be attributed to suppression of PET due to the formation of the ‘‘free’’ ion pair by proton-transfer reactions. Laser confocal microscope experiment shows the potential utilization of CDs-imidazole for the probed proton-transfer reactions in living cells. This study shows not only great potential of the present CDs-imidazole in analytical chemistry, photochemistry and photophysics, but also their potential applications to environmental monitoring systems in industry.

Dalton Transactions Accepted Manuscript

Acknowledgments

The authors would like to thank the Natural Science Foundation of China (no. 21271094). This work was supported by the National Science Foundation for Fostering Talents in Basic Research of the National Natural Science Foundation of China (Grant no. J1103307).

References

1 N. Karousis, N. Tagmatarchis and D. Tasis, *Chem. Rev.*, 2010, **110**, 5366-5397.

2 C.-Z. Li, H.-L. Yip and A. K.-Y. Jen, *J. Mater. Chem.,* 2012, **22**, 4161-4177.

3 R. Nair, P. Blake, A. Grigorenko, K. Novoselov, T. Booth, T. Stauber, N. Peres and A. Geim, *Science*, 2008, **320**, 1308-1308.

4 K. P. De Jong and J. W. Geus, *Catal. Rev.*, 2000, **42**, 481-510.

5 N. Chen, Y. He, Y. Su, X. Li, Q. Huang, H. Wang, X. Zhang, R. Tai and C. Fan, *Biomaterials*, 2012, **33**, 1238-1244.

6 S. N. Baker and G. A. Baker, *Angew. Chem., Int. Ed.,* 2010, **49**, 6726-6744.

7 H. Jiang, F. Chen, M. G. Lagally and F. S. Denes, *Langmuir*, 2009, **26**, 1991-1995.

8 S.-L. Hu, K.-Y. Niu, J. Sun, J. Yang, N.-Q. Zhao and X.-W. Du, *J. Mater. Chem.*, 2009, **19**, 484-488.

9 H. Li, X. He, Z. Kang, H. Huang, Y. Liu, J. Liu, S. Lian, C. H. A. Tsang, X. Yang and S. T. Lee, *Angew. Chem., Int. Ed.*, 2010, **49**, 4430-4434.

10 A. B. Bourlinos, A. Stassinopoulos, D. Anglos, R. Zboril, V. Georgakilas and E. P. Giannelis, *Chem. Mater.*, 2008, **20**, 4539-4541.

11 A. B. Bourlinos, A. Stassinopoulos, D. Anglos, R. Zboril, M. Karakassides and E. P. Giannelis, *Small*, 2008, **4**, 455-458.

Dalton Transactions Accepted Manuscript

12 R. Liu, D. Wu, S. Liu, K. Koynov, W. Knoll and Q. Li, *Angew. Chem.*, 2009, **121**, 4668-4671.

13 H. Zhu, X. Wang, Y. Li, Z. Wang, F. Yang and X. Yang, *Chem. Commun.*, 2009, 5118-5120.

14 C. Liu, P. Zhang, F. Tian, W. Li, F. Li and W. Liu, *J. Mater. Chem.*, 2011, **21**, 13163-13167.

15 Y. Fang, S. Guo, D. Li, C. Zhu, W. Ren, S. Dong and E. Wang, *ACS Nano*, 2011, **6**, 400-409.

16 S. Zhu, S. Tang, J. Zhang and B. Yang, *Chem. commun.*, 2012, **48**, 4527-4539.

17 D. Wang, X. Wang, Y. Guo, W. Liu and W. Qin, *RSC Adv.*, 2014, **4**, 51658-51665.

18 S. Zhuo, M. Shao and S.-T. Lee, *ACS Nano*, 2012, **6**, 1059-1064.

19 H. Li, Y. Zhang, L. Wang, J. Tian and X. Sun, *Chem. Commun.*, 2010, **47**, 961-963.

20 H. M. Gonçalves, A. J. Duarte and J. C. Esteves da Silva, *Biosens. Bioelectron.*, 2010, **26**, 1302-1306.

21 H. X. Zhao, L. Q. Liu, Z. De Liu, Y. Wang, X. J. Zhao and C. Z. Huang, *Chem. Commun.*, 2011, **47**, 2604-2606.

22 L. Tang, R. Ji, X. Cao, J. Lin, H. Jiang, X. Li, K. S. Teng, C. M. Luk, S. Zeng and J. Hao, *ACS Nano*, 2012, **6**, 5102-5110.

23 Y. Dong, R. Wang, G. Li, C. Chen, Y. Chi and G. Chen, *Anal. Chem.*, 2012, **84**, 6220-6224.

24 W. Shi, X. Li and H. Ma, *Angew. Chem.*, 2012, **124**, 6538-6541.

25 M. M. Choi and D. Xiao, *Anal. Chim. Acta*, 1999, **387**, 197-205.

26 Y. Ooyama, K. Uenaka, A. Matsugasako, Y. Harima and J. Ohshita, *RSC Adv.*, 2013, **3**, 23255-23263.

27 Y. Ooyama, H. Egawa and K. Yoshida, *Dyes Pigments*, 2009, **82**, 58-64.

28 N. Boens, W. Qin, M. Baruah, W. M. De Borggraeve, A. Filarowski, N. Smisdom, M. Ameloot, L. Crovetto, E. M. Talavera and J. M. Alvarez‐Pez, *Chem. - Eur. J.*, 2011, **17**, 10924-10934.

Dalton Transactions Accepted Manuscript

29 Z. Zhang, Y. Shi, Y. Pan, X. Cheng, L. Zhang, J. Chen, M.-J. Li and Y. Changqing, *J. Mater. Chem. B*, 2014.

30 J. C. de Mello, H. F. Wittmann and R. H. Friend, *Adv. Mater.*, 1997, **9**, 230-232.

31 D. O'Connor, *Time-correlated single photon counting*, Academic Press, 1984.

32 N. Boens, W. Qin, N. Basaric, J. Hofkens, M. Ameloot, J. Pouget, J.-P. Lefevre, B. Valeur, E. Gratton and M. VandeVen, *Anal. Chem.*, 2007, **79**, 2137-2149.

33 D. Wang, Y. Guo, W. Liu and W. Qin, *RSC Adv.*, 2014, **4**, 7435-7439.

34 S. Qu, X. Wang, Q. Lu, X. Liu and L. Wang, *Angew. Chem.*, 2012, **124**, 12381-12384.

35 X. Jia, J. Li and E. Wang, *Nanoscale*, 2012, **4**, 5572-5575.

36 Z. Lin, W. Xue, H. Chen and J.-M. Lin, *Anal. Chem.*, 2011, **83**, 8245-8251.

37 N. Agmon, *Chem. Phys. Lett.*, 1995, **244**, 456-462.

38 M. Eigen, *Angew. Chem., Int. Ed.*, 1964, **3**, 1-19.

39 T. Kumpulainen and A. M. Brouwer, *Phys. Chem. Chem. Phys.*, 2012, **14**, 13019-13026.

40 S. Silvi, A. Arduini, A. Pochini, A. Secchi, M. Tomasulo, F. M. Raymo, M. Baroncini and A. Credi, *J. Am. Chem. Soc.*, 2007, **129**, 13378-13379.

41 D. Spry, A. Goun, K. Glusac, D. E. Moilanen and M. Fayer, *J. Am. Chem. Soc.*, 2007, **129**, 8122-8130.

42 D. Stoner-Ma, A. A. Jaye, P. Matousek, M. Towrie, S. R. Meech and P. J. Tonge, *J. Am. Chem. Soc.*, 2005, **127**, 2864-2865.

43 E. C. Carroll, S.-H. Song, M. Kumauchi, I. H. van Stokkum, A. Jailaubekov, W. D. Hoff and D. S. Larsen, *J. Phys. Chem. Lett.*, 2010, **1**, 2793-2799.

44 M. Kamiya, S. Saito and I. Ohmine, *J. Phys. Chem. B*, 2007, **111**, 2948-2956.

Dalton Transactions Accepted Manuscript

Dalton Transactions Accepted Manuscript

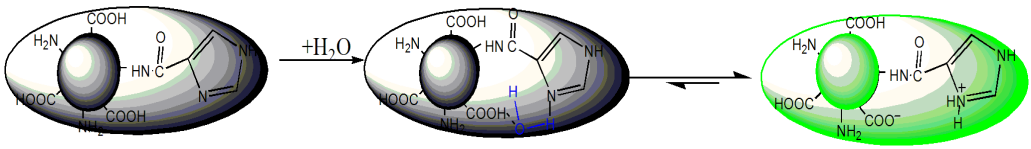

Non fluorescence

Strong fluorescence

Dalton Transactions Accepted Manuscript